Quasicrystalline coatings through laser processing: A study on process optimisation and microstructure evolution.

K.Chattopadhyay, K.Biswas, S.Bysakh, G.Phanikumar
Department of Metallurgy
Indian Institute of Science
Bangalore 560012, India
and
A.Weisheit, R.Galun and B.Mordike
IWW, Technical University of Clausthal
Clausthal-Zellerfeld, Germany

ABSTRACT

Composite coatings containing quasicrystalline (QC) phases in Al-Cu-Fe alloys were prepared by laser cladding using a mixture of the elemental powders. Two substrates, namely pure aluminum and an Al-Si alloy were used. The clad layers were remelted at different scanning velocities to alter the growth conditions of different phases. The process parameters were optimized to produce quasicrystalline phases. The evolution of the microstructure in the coating layer was characterized by detailed microstructural investigation. The results indicate presence of quasicrystals in the aluminum substrate. However, only approximant phase could be observed in the substrate of Al-Si alloys. It is shown that there is a significant transport of Si atoms from the substrate to the clad layer during the cladding and remelting process. The hardness profiles of coatings on aluminum substrate indicate a very high hardness. The coating on Al-Si alloy, on the other hand, is ductile and soft. The fracture toughness of the hard coating on aluminum was obtained by nano-indentation technique. The K_{1C} value was found to be 1.33 MPa $m^{1/2}$ which is typical of brittle materials.

INTRODUCTION

After the discovery of quasicrystals by Shectman et al. in 1984 [1], it took almost ten years to make these new materials industrially useful. The application of quasicrystals is thought of only after the discovery of stable quasicrystalline systems [2]. These materials exhibit attractive properties such as high hardness [3], low thermal conductivity [4], low density, good oxidation and corrosion resistance [5] and low fiction coefficient [6]. Consequently, these materials are found to be potential candidates for various applications such as wear resistant coatings on ductile materials [7], thermal barrier coatings [4], thermoelectric materials [8]. The QC coated nonstick cookware [9] and high strength maraging steels [10] developed by Sandvik steels are already in the market. QC coating has already been tested as thermal barrier coating in aircraft engines [11].

Laser cladding has been extensively used to obtain wear and corrosion resistant coating on different substrates [12]. Laser cladding involves formation of coating by melting the coating material along with a thin layer of substrate with a high power laser beam normal to the surface. Coating forms due to rapid solidification of the melt with material build up on the substrate. There is very few literatures available on laser cladding of quasicrystalline materials. The first

research work on quasicrystalline phase formation by laser melting of ingots of Al-Cu-Fe was reported by Baumeister et al [13]. Auderbert et al. [14] have shown that it possible to produce quasicrystalline phases by laser cladding of aluminum base alloys using elemental powder mix.

Our study focuses on quasicrystalline coating of Al-Cu-Fe system by laser cladding using elemental powder mix of Al, Cu and Fe on Al and Al-10.5 at% Si substrates. Using a powder mix of composition close to $Al_{65}Cu_{20}Fe_{15}$, laser clads were prepared at two different scan speeds. Some of the clads were remelted to see the effect of remelting on quasicrystalline phase formation. The study also deals with the optimisation of process as far as composition of powder mix and laser scan rates are concerned. One of the aims of the present study is to correlate the microstructure with properties.

EXPERIMENTAL PROCEDURE

Clads were prepared using CO_2 laser with following parameters:

Power = 3 kW
Dia. Of Laser Beam = 5 mm
Feed Rate of Powder = 2 gm/min.
Carrier Gas Flow Rate = 6 lit./min.

They were prepared using powder mix of aluminium, copper and iron with nominal composition $Al_{65}(Cu + Fe)_{35}$ with Cu/Fe = 2 and Cu/Fe =1.559/1. The optimized scan rates for cladding were 300 and 600 mm/min. The subsequent remelting experiments were done employing scan rates varying from 600 to 1200 mm/min. The substrate was sand blast in all cases prior to the cladding experiments.

Structural analysis of clads was performed using a JEOL X-ray diffraction machine with $Cu_{k\alpha}(\lambda = 1.5402\ A^o)$. The clad layers were also investigated using scanning electron and transmission microscopes (JEOL JSM 840A and JEOL 2000FXII). The compositions at various positions inside the clads were measured using EDAX analyser attached with SEM. The hardness profiles of the clads were measured using Shimadzu 2000 microhardness tester with a load of 25g. A nanoindentation measurement using 200 mN load and Berkovich Indentor technique was used to arrive at the fracture toughness of the clad layer.

RESULTS

Al-Cu -Fe Coating on Al substrate

The composition of the powder mix is found to be the most important variable in icosahedral phase formation in the clads. Figure 1 shows the effect of powder composition on the phase formation. The XRD pattern of clad with powder composition $Al_{65}(Cu+Fe)_{35}$ with Cu/Fe =1.559/1 is shown in figure 1a. It shows no icosahedral phase (I phase) peaks. Intermetallic phases Fe_3Al and $CuAl_2$ can be detected. The corresponding composition profile (figure 1b) shows that Cu content is less in the clad layer than is required for I –phase formation.

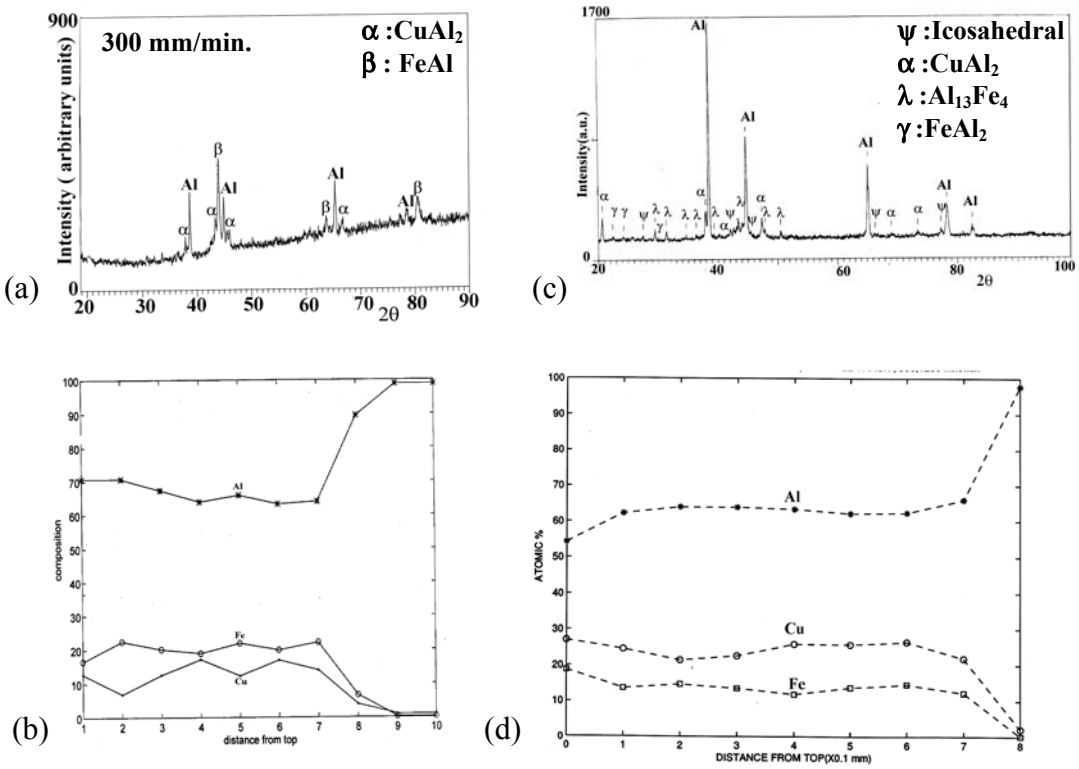

Figure 1 : The effect of powder compositions on the quasicrystalline phase formation on Al substrate: (a) XRD pattern and (b) EDAX analysis of powder $Al_{65}(Cu+Fe)_{35}$ with Cu/Fe =1.559 (c) XRD pattern and (d) EDAX analysis of powder $Al_{65}(Cu+Fe)_{35}$ with Cu/Fe =2.0

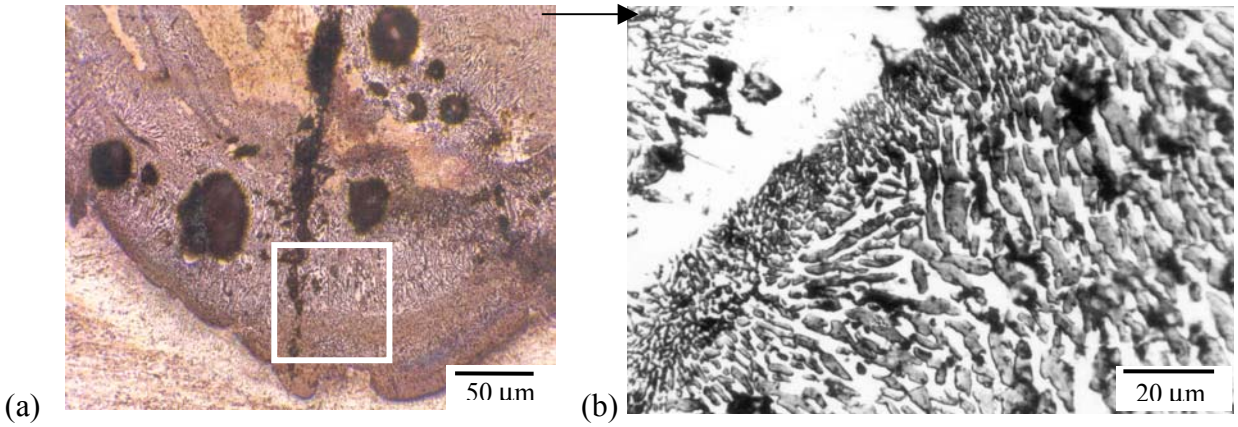

Figure 2. Typical optical micrographs of laser clad $Al_{65}(Cu+Fe)_{35}$ with Cu/Fe=2.0 on Al substrate. (a) low magnification (b) high magnification.

The figure1c and 1d shows the XRD pattern and corresponding composition profile of the clad with composition $Al_{65}(Cu + Fe)_{35}$ with Cu/Fe = 2/1 with scan rate of 600 mm/min. In both the cases I –phase has formed in the clad along with monoclinic $Al_{13}Fe_4$ and $CuAl_2$ phases. Although, the AlFe(β) phase can be detected in fig.1b, it is present in minute quantity. The composition profiles show that proportions of the constituent elements is in the I-phase formation range. The figure 2a shows low magnification micrograph of a clad. The area is chosen to highlight the nature of process related defects. It can be seen that it contains varying amounts of pores and cracks. The high magnification micrograph (fig. 2b) shows two phase microstructure in the clad pool. The microstructure varies along the depth of the clad pool, being finer at top due to remelting**.**

Figure 3 shows the SEM micrograph inside the clad. The micrograph shows typical dendritic morphology. Three distinct phases can be detected with white, dark and gray contrasts. The composition analysis by EDAX shows the gray areas consist of icosahedral phase with composition $Al_{67.5}Cu_{15}Fe_{17.5}$.The dark areas are found to have composition $Al_{68.8}Fe_{22}Cu_{9.2}$, which is very close to $Al_{13}Fe_4$.The white areas show composition close to $CuAl_2$ ($Al_{67}Cu_{29}Fe_4$). In order to identify conclusively the presence of different phases and their distribution, a detailed transmission electron microscopic characterization has been carried out. The typical bright field micrograph shows the presence of dendritic morphology of phases in the clad pool. The long dendrites are found to be $(Al,Cu)_{13}Fe_4(\lambda)$ as can be seen from figure 4a showing the diffraction pattern taken along [243] zone axis. These dendrites are heavily twinned. The figure 4b shows four different twinned variants. The presence of the icosahedral phase can be detected from the microdiffraction pattern taken along 5-fold direction shown in figure 5. The fivefold axis of icosahedral phase grows along [010] direction of λ phase in accordance with the earlier results [14]. Presence of the decagonal phase can be detected from the microdiffraction pattern taken along 10-fold direction as shown in figure 6.

The hardness profile of a typical track is shown in figure 7. The hardness profile shows a constant hardness of 650 VHN in all tracks. The hardness level is higher than what is reported in the literature [14]. This is mainly because of the presence of other intermetallic phases ($Al_{13}Fe_4$,$CuAl_2$.). The hardness varies with distance because of presence of these phases.

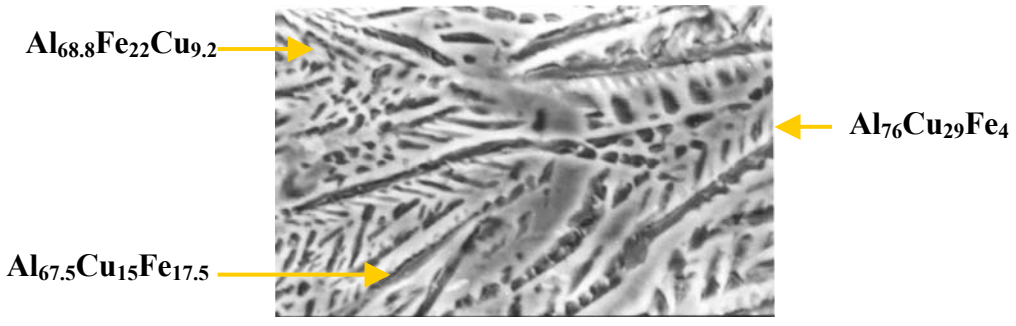

Figure 3. SEM Micrograph with compositions of various phases determined by EDAX in $Al_{65}(Cu+F2)_{35}$ with Cu/Fe=2.0 on Al substrate.

Al-Cu-Fe coating on Al-Si substrate

The figure 8 shows the X-ray diffractograms for this coating for both clad (scan speed: 300 mm/min.) and remelted (300 mm/min followed by 1000 mm/min) tracks. Both the tracks contain

icosahedral phase along with $(Al,Cu)_{13}Fe_4$ and $CuAl_2$ phases. It can be found that the remelted tracks show more peaks of icosahedral phase than the clad layer. This indicates that remelting improves the formation of icosahedral phase. The figure 9 shows the composition profile of the remelted track, showing high amount of Al (70-80 at%) and Si (8-11 at%) and low amount of Cu and Fe in the pool compared to the cases for Al substrate. In these tracks, we have used powder composition of Al_{65} $(Cu + Fe)_{35}$ with Cu/Fe =2/1. Therefore, the extra Al and Si have come from the substrate during cladding and remelting. The optical micrograph (figure 10a) shows two distinct layer, which can be treated as cladded and remeted layer. The clad layer shows dendritic morphology but the remelted layer shows finer microstructure containing much finer dendritic precipitates. The scanning electron micrographs (figure 10b) of the remelted region at low magnification reveals growth shapes of this phase. The high magnification micrographs show that these precipitates are five fold dendrites, which is very typical for icosahedral phase. The EDAX analysis shows that these dendrites have typical composition $Al_{67}Si_{10}Cu_{6.5}Fe_{16.5}$. The interdedritic regions is found to be containing mainly Al (73 at %) and Si (13 at %). Some of the dendrites are broken. The dendrites of four fold, six fold symmetry can also be found in the remelted layer. The clad layer shows the presence of long dendrites. The compositional analysis shows these dendrites have composition very close to $(Al,Cu)_{13}Fe_4$ i.e., $(Al_{67}Cu_5Fe_{26})$. The characterization by TEM has shown that the five fold dendrites in the remelted layer are 1/1 cubic rational approximants of the icosahedral phase. The figure 11 shows the [001], [011] and [111] zone axis patterns conclusively establishing the phase to be a rational approximant with body centre cubic structure. Lee et al.[15] have shown that the Si addition beyond 5 at % stabilizes the 1/1 cubic rational approximant to icosahedral phase in this system.

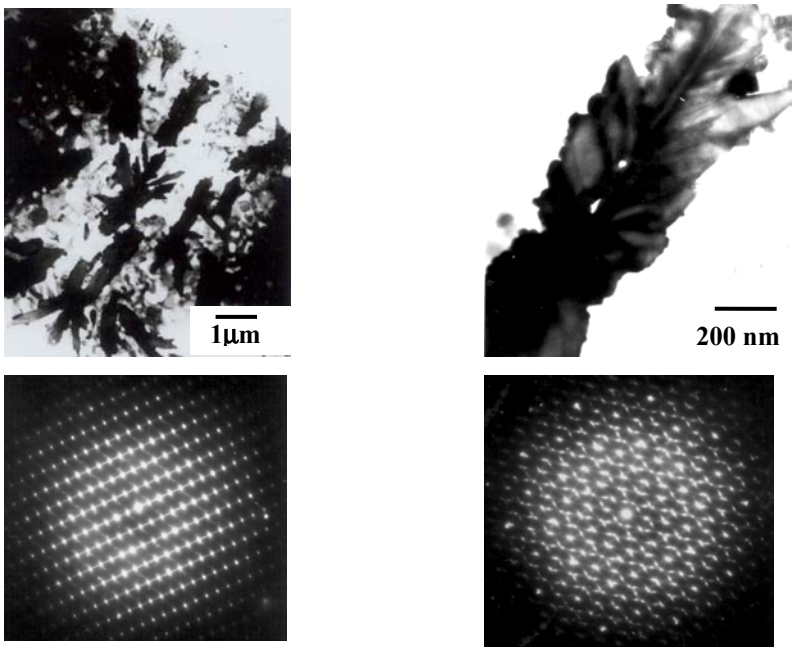

Figure 4. The [243] zone axis pattern of $(Al, Cu)_{13}Fe_4$ and its twinned variants in $Al_{65}(Cu+Fe)_{35}$ with Cu/Fe=2 on Al substrate.

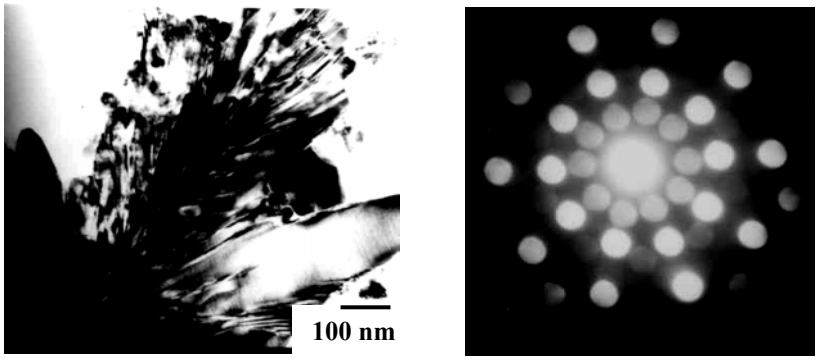

Figure 5. The icosahedral phase particle with typical five fold pattern.

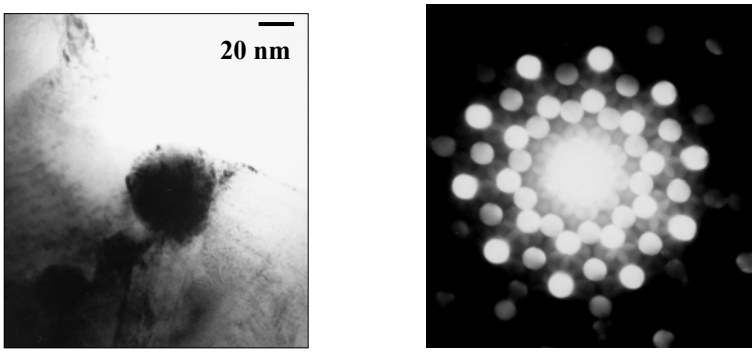

Figure 6. Nanometer size decagonal particle and corresponding microdiffraction pattern in clad $Al_{65}(Cu+Fe)_{35}$ with Cu/Fe=2.0 on Al substrate.

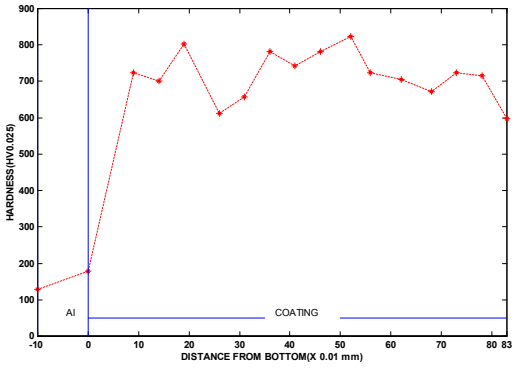

Figure 7. Hardness profile of coating, clad at 300 mm/min.and remelted at 600 mm/min on Al substrate.

The lattice parameter of rational approximant p/q can be given by

$$a_{\frac{p}{q}} = \frac{2(q\tau + p)a_R}{\sqrt{2+\tau}}$$

where a_R is the quasilattice constant. Using quasilattice constant (a_R) for Al-Cu-Fe-Si system as 0.0447 nm (Tsai et al.[16]) we get $a_{1/1}$ = 1.23 nm. From the [001] zone axis pattern, it can be calculated that a_R = 1.23 nm, which shows a perfect match between the theoretical and experimental analysis.

The most interesting fact is that the diffraction patterns taken along various zone axes show the diffuse intensity .The EDPs along [001] and [011] show the diffuse intensity in the form of deformed rings. The rings are found located in the reciprocal lattice in zero order Laue zone. The diffuse scattering centers on reflections forbidden by Im3 space group. The diffuse intensity contours center at $\left(\frac{1}{2}\frac{1}{2}\frac{1}{2}\right)$ positions and pass through $\left(\pm\frac{1}{3}\pm\frac{1}{3}\pm\frac{1}{3}\right)$ positions. The diffuse intensity is not homogeneously distributed but reinforcement occurs along segment connecting $\left(\pm\frac{1}{3}\pm\frac{1}{3}\pm\frac{1}{3}\right)$ type positions.

A typical hardness profile is shown in figure 12. The hardness is high in the middle of the pool but quite low at the top layer, which indicates the Si addition makes the coating soft and deformable. The high hardness in the middle of the pool indicates the presence of some intermetallic phases as shown by the EDAX analysis.

Attempts are made to evaluate the fracture toughness of the clad layers on Al and Al-Si substrates by a combination of crack length measurements from the indentation and determination of the modulus of the composite layer by nanoindentation technique. The typical nanoindentation curve for the clad on aluminum substrate is shown in figure 13. It is possible to evaluate the modulus if we assume a poisson ratio of 0.3 [18]. The fracture toughness was determined from the expression [19]:

$$K_{IC} = \xi\left(\frac{E}{H}\right)^{\frac{1}{2}}\left(\frac{P}{C^{\frac{3}{2}}}\right)$$

where P = Load, 2c = crack length , E = Elastic Modulus, H = Vicker's Hardness, ζ = 0.016

(a) 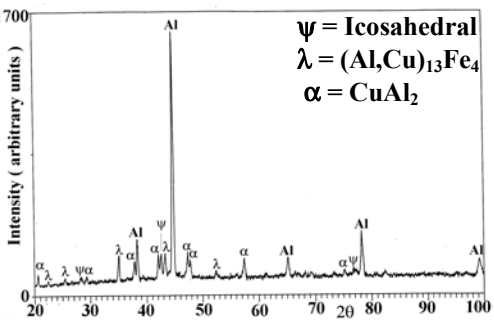

(b) 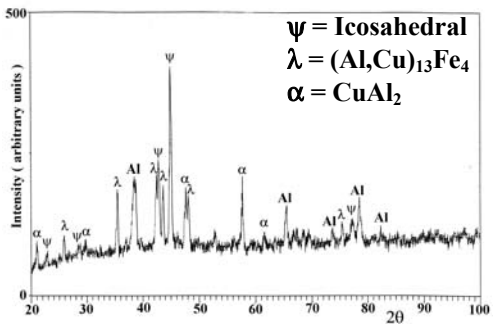

Figure 8. The XRD patterns : (a) clad at 300 mm/min (b) clad at 300 mm/min. and remelted at 1000 mm/min. The substrate is Al-10.5 at%Si.

DISCUSSION

The phase evolution in the Al–Cu–Fe system is complex. Both icosahedral and decagonal phase forms although decagonal has only metastable existence. The icosahedral phase is thermodynamically stable [2]. The icosahedral phase formation depends on solidification rate [15]. At slow to moderate (~1 ^{o}C/sec. to 10^{2} ^{o}C/sec.) the I-phase forms by peritectic reaction between liquid and monoclinic $Al_{13}Fe_4$ or $(Al,Cu)_{13}Fe_4(\lambda)$ at 875^{o}C.

$$L + \lambda \rightarrow I(Al_{65}Cu_{20}Fe_{15}) \quad \text{.....(a)}$$

The primary λ nucleates directly from the liquid and grows in the liquid and β phase(AlFe) based on CsCl structure forms by another peritectic reaction between liquid and λ.

$$L + \lambda \rightarrow \beta \quad \text{.....(b)}$$

At very high cooling rate (~10^{6} ^{o}C/sec) the I-phase forms directly from liquid without the formation of crystalline phases. The XRD analysis shows the presence of icosahedral phase with λ. The $CuAl_2$ forms much later from the liquid as dendrites. The composition analysis by EDAX shows the same type of solidification morphology. The composition of different phases indicates that the I-phase forms by the peritectic reaction between liquid and solid phase λ. The TEM analysis shows the presence of λ as big dendrite and I-phase forms at the ends of the long dendrite arms. The presence of $CuAl_2$ is also corroborated by TEM study. $CuAl_2$ forms at the end of the solidification path.

The phase formation is different in the case of Al-Si substrate due to Si transport in to the clad layer from the substrate. We have shown exact correspondence of the I-phase in the XRD results. However, TEM observations show that 1/1 cubic approximant phase is the major constituent in the remelted layer. It has been mentioned [17] that when Si is added more that 2 at%, the cubic phase can form over a large domain of compositions and temperatures. It has been found from EDAX analysis that the Si content in remelted layer of all clads on the Al-Si substrate is 8- 10 at%. This amount of Si has come from the substrate during remelting and it stabilizes the cubic phase. One of the major results of the present investigation is very high hardness of the clad of the quasicrystal composition on aluminum substrate. Since the volume fraction of QC is not large, the results show significant contribution from the approximant λ phase.

Surprisingly, the formation of the 1/1 cubic rational approximant in the remelted layer of Al-Si substrate reduces the hardness and imparts significant ductility to the clad layer. The fracture toughness of the clad region on the Al substrate (K_{1C}= 1.32 MPa $m^{1/2}$) is similar to that observed in brittle materials like silicon and may not be acceptable in actual use. However, an opportunity exists for producing a QC composite with 1/1 ductile approximant phase to improve the fracture toughness of the clad layer.

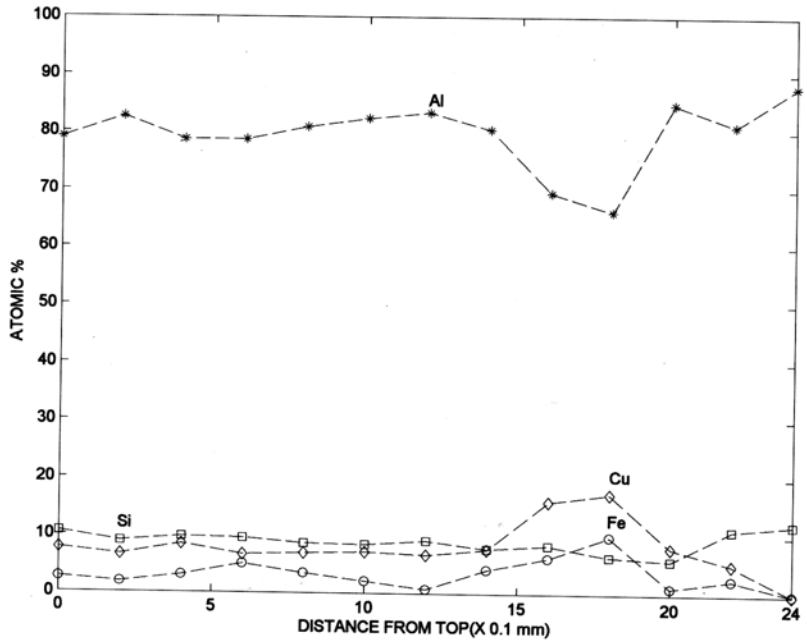

Figure 9. Composition profile of track : Cladding : 300mm/min . Remelting : 500 mm/min.

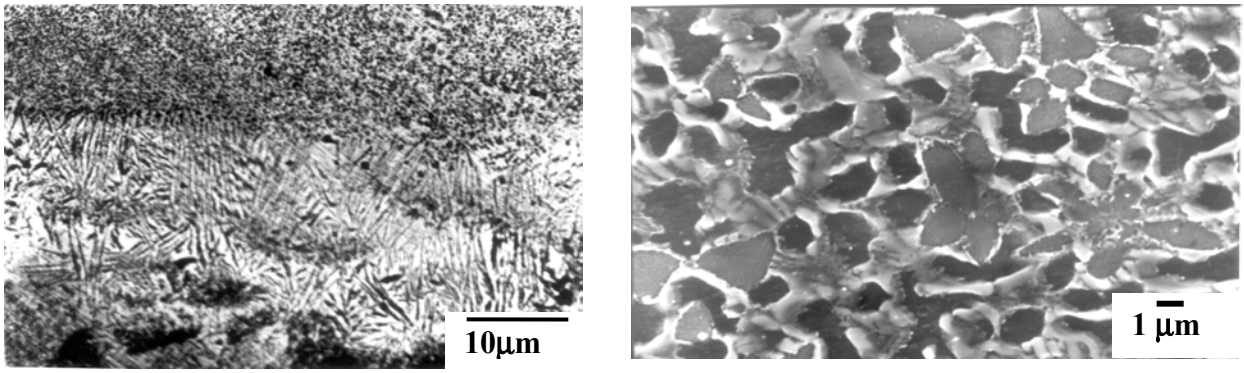

(a) **(b)**

Figure 10. (a) Optical micrograph of clad pool and (b)SEM micrograph of clad layer cladding: 300 mm/min. and remelting: 1000 mm/min.

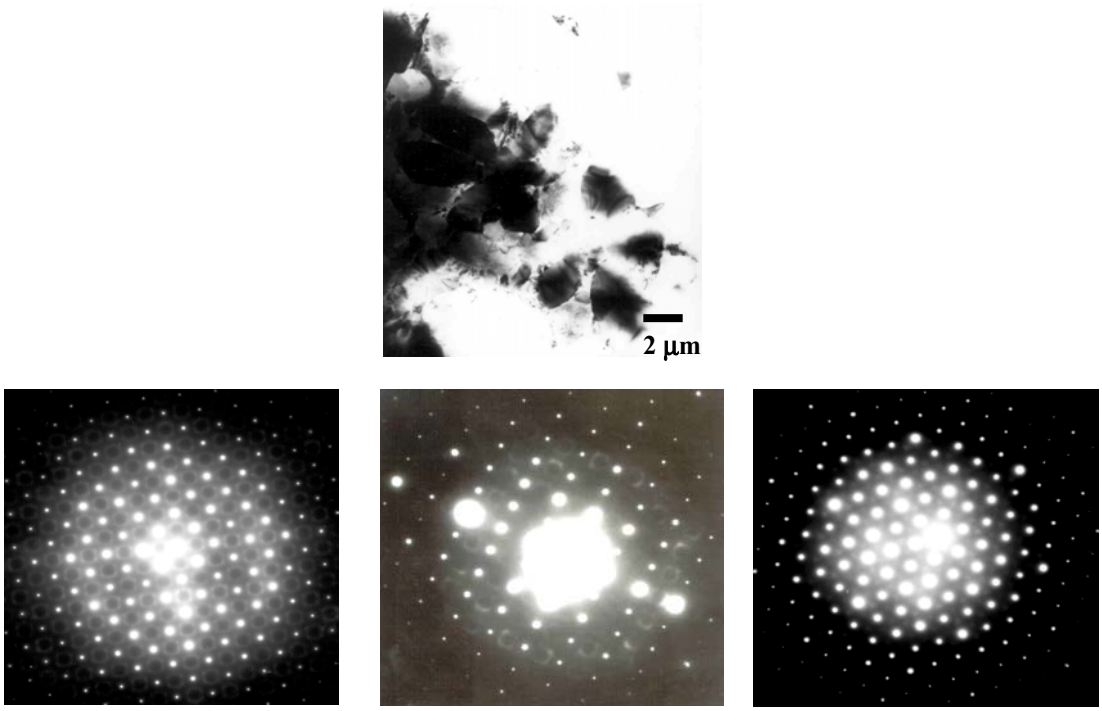

(a) (b) (c)

Figure 11. The bright field micrograph and corresponding [001], [011] and $[11\bar{1}]$ zone axis patterns of 1/1 cubic rational approximant in the clad layer on Al-10.5 at%Si substrate.

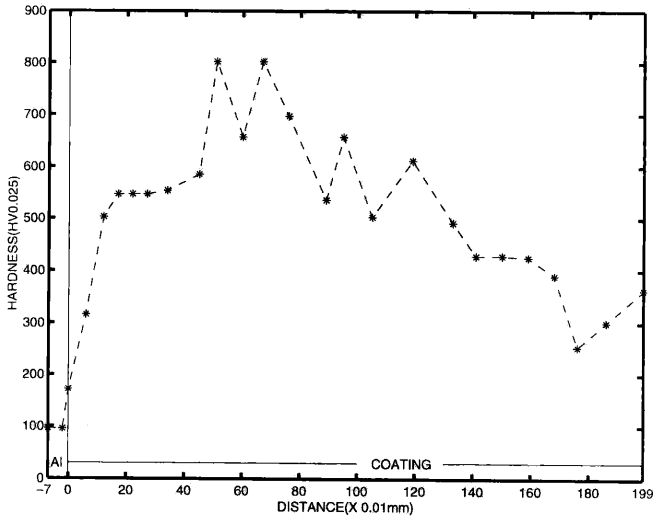

Figure 12. Hardness profile for a clad on Al-10.5 at% Si with scan speed of 300 mm/min. and remelting speed of 1000 mm/min.

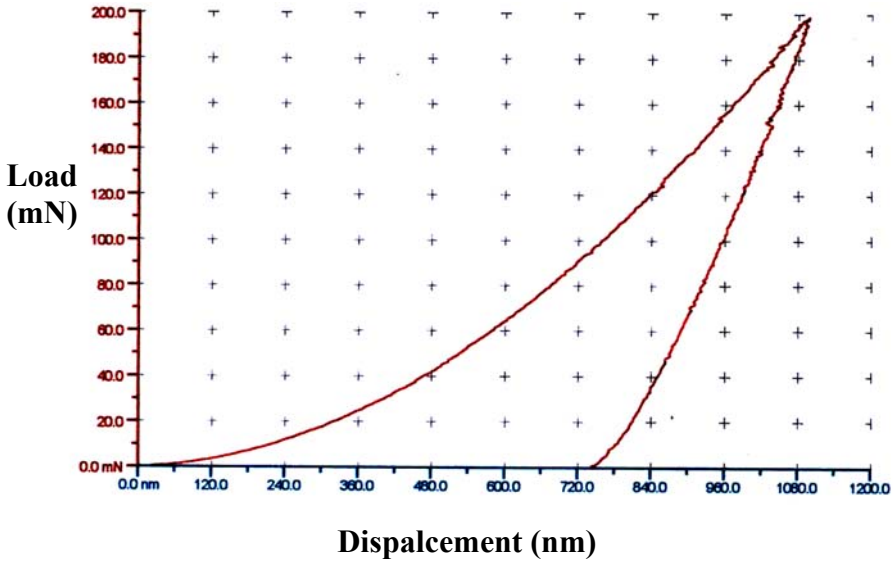

Figure 13. Nano-indentation plot of QC coating on Al substrate, clad at 600 mm/min.

ACKNOWLEDGEMENT

Funding for this work was through collaborative Indo-German programmes by BHBF and Volkswagon Foundation. The support of CSIR, India towards the Indian investigators is also acknowledged. The authors like to thank Dr. Rajan, Head, Surface Engineering Division, National Aerospace Laboratories, Bangalore, India for helping in conducting nanoindentation measurements.

REFERENCES

1. D. Schectman, I. Blech, D. Gratias, J.W.Cahn, Phys. Rev. Lett. 53(20),1951 (1984)
2. A. P. Tsai, A. Inoue, and T. Masumoto, Jpn. J. App. Phys.26, L1505 (1987)
3. S. S. Kang, J. M. Dubois, and J. von. Stebut, J. Mate. Res.,8, .2471 (1993)
4. P. Archambault and C. Janot, MRS Bull. 22,.48 (1997)
5. M. F.Basser and T. Eisenhammer, MRS Bull. 22,.59 (1997)
6. D. J. Sordelet and J. M. Dubois, MRS Bull., 22,.34 (1997)
7. J. M. Dubois, S.S.Kang and A. Perrot, Mater. Sc. and Engg. A179,122 (1994)
8. T. M. Tritt, Science, 283, 804 (1999)
9. J. M. Dubois, S.S.Kang and J. von. Stebut, J.Mater. Sc.Lett, 10, 537 (1991)
10. P. Liu, A.H. Stigenberg and J.-O. Nilson, Acta Metall.Meter.,43(7), 2881 (1995)
11. Industries de Techniques (French Publication) 784, 17 (1997)
12. R. Vilar, J. Laser Applications, 11 (2),64 (1999)
13. G.Baumeister, Birgit Skrotzki and Gunther Eggler, Prakt. Metallogr.34,.8, (1997),

14. F. Audebert, R. Colaco, R. Viller and H. Sirkin, Scripta. Mater., 40(5), 551 (1999)
15. S.M. Lee, B.H. Kim, W.T. Kim and D.H. Kim, Materials Science and Engineering (in press).
16.A.P. Tsai,. A. Inoue, and T. Masumoto, J. of Mat. Sci. Letts 8, 470 (1989)
17. A. Quivy, M.Quiquandon, Y.Calvayrac., F.Faudot, D.Gratias, C.Berger, R.A.Brands, V.Simnonet, and F. Hippert, J.Phys. Condens..Matter., 8, 4223 (1996)
18. Y. Yokoyama, A.Inoue and T.Masumoto , Mater. Trans. JIM 34 , 135 (1993)
19. G.R Anstis, P Chantikul, B.R Lawn and D.B Marshall, J. Am. Ceram. Soc., 64, 533 (1981).